Title	Functional Roles of Phase Resetting in the Gait Transition of a Biped Robot From Quadrupedal to Bipedal Locomotion
Author(s)	Aoi, Shinya; Egi, Yoshimasa; Sugimoto, Ryuichi; Yamashita, Tsuyoshi; Fujiki, Soichiro; Tsuchiya, Kazuo
Citation	IEEE Transactions on Robotics (2012), 28(6): 1244-1259
Issue Date	2012-12
URL	http://hdl.handle.net/2433/167746
Right	© 2012 IEEE. Personal use of this material is permitted. Permission from IEEE must be obtained for all other uses, in any current or future media, including reprinting/republishing this material for advertising or promotional purposes, creating new collective works, for resale or redistribution to servers or lists, or reuse of any copyrighted component of this work in other works.
Type	Journal Article
Textversion	author

Functional roles of phase resetting in the gait transition of a biped robot from quadrupedal to bipedal locomotion

Shinya Aoi, *Member, IEEE*, Yoshimasa Egi, Ryuichi Sugimoto, Tsuyoshi Yamashita, Soichiro Fujiki, and Kazuo Tsuchiya

***Abstract*—Although physiological studies have shown evidence of phase resetting during fictive locomotion, the functional roles of phase resetting in actual locomotion remain largely unclear. In this paper, we constructed a control system for a biped robot based on physiological findings and investigated the functional roles of phase resetting in the gait transition from quadrupedal to bipedal locomotion by numerical simulations and experiments. So far, although many studies have investigated methods to achieve stable locomotor behaviors for various gait patterns of legged robots, their transitions have not been thoroughly examined. Especially, the gait transition from quadrupedal to bipedal requires drastic changes in the robot posture and the reduction of the number of supporting limbs, and so the stability greatly changes during the transition. Thus, this transition poses a challenging task. We constructed a locomotion control system using an oscillator network model based on a two-layer hierarchical network model of a central pattern generator while incorporating the phase resetting mechanism, and created robot motions for the gait transition based on the physiological concept of synergies. Our results, which demonstrate that phase resetting increases the robustness in gait transition, will contribute to the understanding of the phase resetting mechanism in biological systems and lead to a guiding principle for designing control systems for legged robots.**

***Index Terms*—Biped robot, Gait transition, Quadrupedal and bipedal, Central pattern generator, Phase resetting, Synergy.**

I. Introduction

Humans and animals achieve adaptive walking in diverse environments by cooperatively and skillfully manipulating their complicated and redundant musculoskeletal systems. They walk on level ground, up and down slopes, at fast and slow speeds, and turn left and right. Some animals crawl, walk quadrupedally or bipedally, run, hop, leap, and jump, depending on the situation.

To clarify the neuro-control mechanisms producing such adaptive locomotor behaviors, many studies have been conducted. Physiological studies have greatly helped to elucidate locomotor mechanisms by examining the configurations and activities of neural systems [35], [60], [68], [76], [81]. However, it is difficult to fully clarify the mechanisms in terms of the nervous system alone because locomotion is a well-organized motion generated through dynamic interactions of the body, its nervous system, and the environment. To overcome such limitations, constructive approaches using computer simulations and robots have recently attracted attention. Because researchers have learned to construct reasonably realistic models of the musculoskeletal and nervous systems, simulations have been performed to investigate neuromechanical interactions [4], [10], [40], [61], [78–80], [86], [87]. In addition to computer simulations, robots have become effective tools for testing hypotheses of locomotor mechanisms and control systems by demonstrating real-world dynamic characteristics [5], [6], [19], [23], [27], [29], [33], [39], [44], [48], [56], [62], [67].

Physiological evidence suggests that central pattern generators (CPGs) in the spinal cord strongly contribute to rhythmic limb movement, such as locomotion [35], [60], [76]. The CPGs can produce oscillatory behaviors even without rhythmic input and proprioceptive feedback. However, they must use sensory feedback to produce effective locomotor behavior. Physiological studies have shown that locomotor rhythm and its phase are modulated by producing phase shift and rhythm resetting based on sensory afferents and perturbations (phase resetting) [17], [26], [36], [46], [74]. However, such rhythm and phase modulations in phase resetting have for the most part been investigated during fictive locomotion in cats, and their functional roles during actual locomotion remain largely unclear. To examine the functional roles of phase resetting during human bipedal locomotion, simulation studies have recently been conducted. These studies demonstrate that phase resetting plays important roles in generating adaptive locomotor behavior [4], [57], [87]. In addition, robotic studies using biped robots have been performed to examine the functional roles of phase resetting during bipedal locomotion by showing real-world dynamic characteristics [5], [6], [55–57].

In this paper, we focus on the investigation of the functional roles of phase resetting in the gait transition of a biped robot from quadrupedal to bipedal locomotion during walking. To establish the gait transition, we have to produce stable walking for both quadrupedal and bipedal locomotion, and in addition, change the robot motions from quadrupedal to bipedal locomotion without falling over. Although many studies have investigated methods to achieve stable locomotor behaviors for various gait patterns, the transitions have not really been

S. Aoi, Y. Egi, R. Sugimoto, T. Yamashita, and S. Fujiki are with the Dept. of Aeronautics and Astronautics, Graduate School of Engineering, Kyoto University, Yoshida-honmachi, Sakyo-ku, Kyoto 606-8501, Japan, email: shinya_aoi@kuaero.kyoto-u.ac.jp

K. Tsuchiya is with the Dept. of Energy and Mechanical Engineering, Faculty of Science and Engineering, Doshisha University, 1-3 Tatara, Miyakodani, Kyotanabe, Kyoto 610-0394, Japan.

S. Aoi and K. Tsuchiya are with JST, CREST, 5 Sanbancho, Chiyoda-ku, Tokyo 102-0075, Japan.

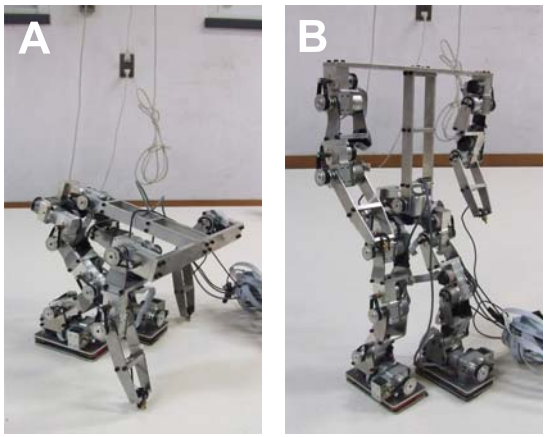

Fig. 1. Biped robot. **A** and **B** show the robot postures for quadrupedal and bipedal locomotion, respectively.

examined. Furthermore, the gait transition from quadrupedal to bipedal requires drastic changes in the robot posture and the reduction of the number of supporting limbs, and so the stability greatly changes during the transition. Proper timing for changing the gait pattern and adequate modulations of the locomotor rhythm and its phase are crucial to achieve the gait transition. These issues indicate that gait transition is a very effective and useful task for investigating the functional roles of phase resetting in locomotion control, as well as being a challenging task in robotic studies. Clarifying these functional roles will contribute to the understanding of the phase resetting mechanism in biological systems. In addition, these issues can lead to a guiding principle for designing control systems for other legged robots, which will be an important contribution to the generalized study of robotics.

This paper is organized as follows: Section 2 introduces our developed biped robot, Sections 3 and 4 address the locomotion control system and the gait transition strategy, respectively, constructed from physiological findings. Section 5 shows the numerical simulation and experimental results, and Section 6 presents the discussion and conclusion.

II. Biped robot

We designed a biped robot that consists of a trunk composed of two parts (upper and lower trunk), a pair of arms composed of two links, and a pair of legs composed of five links (Fig. 1). Figure 2**A** shows the schematic model of the robot. Each link is connected to the others through a rotational joint with a single degree of freedom. To manipulate the legs, the robot has two joints in the hips (roll and pitch), one joint in the knees (pitch), and two joints in the ankles (roll and pitch). To control the arms, it has one joint in the shoulders (pitch) and one joint in the elbows (pitch). For the trunk, it has one joint in the waist (pitch). Each joint has a motor and an encoder to manipulate the angle. Four touch sensors are attached to the corners of the sole of each foot and one touch sensor is attached to the tip of the hand of each arm. Three gyro sensors are installed on the lower trunk, which are used only for monitoring the robot motion relative to the ground and are not used for the controller.

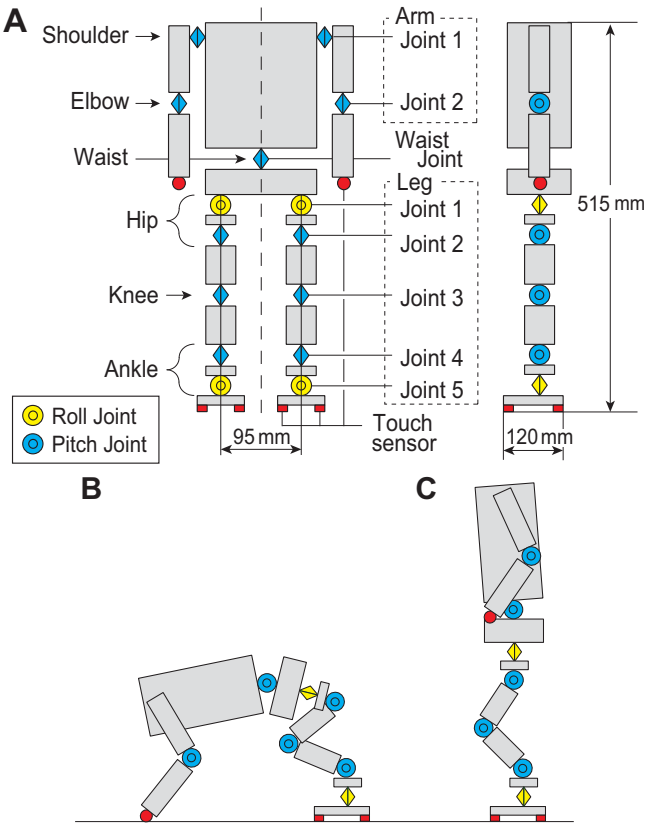

Fig. 2. Schematic models of biped robot. **A** shows front and side views of the robot model. **B** and **C** display its posture during quadrupedal and bipedal walking, respectively.

TABLE I
Physical parameters of the biped robot

Link	Mass [kg]	Length [cm]
Trunk	1.42	27.2
Arm	0.53	22.2
Leg	1.40	24.3
Total	5.28	51.5

The left and right legs are numbered Legs 1 and 2, respectively. The joints of the legs are also numbered: Joints 1 $\cdots$ 5 from the side of the trunk, where Joints 1 and 2 are the roll and pitch hip joints, respectively, Joint 3 is the pitch knee joint, and Joints 4 and 5 are the pitch and roll ankle joints, respectively. The arms are numbered in a similar manner: Joint 1 is the pitch shoulder joint and Joint 2 is the pitch elbow joint. The trunk consists of the upper and lower parts connected by the pitch waist joint, named Waist Joint. To describe the configuration, we introduce angles θ_{W}, $\theta^i_{\mathrm{A}j}$, and $\theta^i_{\mathrm{L}k}$ ($i = 1, 2$, $j = 1, 2$, $k = 1, \ldots, 5$), which are the rotation angles of Waist Joint, Joint j of Arm i, and Joint k of Leg i. The robot walks quadrupedally and bipedally, as shown in Figs. 2**B** and **C**. Table I shows the physical parameters.

The robot walks on a flat floor with no elevation. The electric power is externally supplied and the robot is controlled by an external host computer (Intel Pentium 4 2.8 GHz, RT-Linux), which calculates the desired joint motions and solves the oscillator phase dynamics in the locomotion control system (see Section III). It receives the command signals at intervals of 1 ms. The robot is connected with the electric power unit

and the host computer by cables that are held up during the experiment to avoid influencing the walking behavior.

For the simulation study, we derived the equation of motion using Lagrangian equations as in [10] and solved the equation using the fourth-order Runge-Kutta method with a step size of 1 ms. We used a linear spring and damper system for modeling the ground reaction force. The physical parameters were based on those of our robot, as shown in Table I.

III. Locomotion Control System

A. CPG-based hierarchical network model

Although physiological studies suggest that CPGs greatly contribute to the generation of locomotion and various CPG models have been proposed, the organization of CPGs remains largely uncertain [37], [50]. However, recent physiological findings suggest that CPGs consist of hierarchical networks composed of rhythm generator (RG) and pattern formation (PF) networks [14], [46], [70], [71]. The RG network generates the basic rhythm and alters it by producing phase shifts and rhythm resetting in response to sensory afferents and perturbations (phase resetting). The PF network shapes the rhythm into spatiotemporal patterns of motor commands. CPGs separately control the locomotor rhythm and motor commands in the RG and PF networks, respectively.

In this paper, we constructed the locomotion control system based on a two-layer hierarchical network model composed of the RG and PF models (Fig. 3**A**). With this system, we improved our previous locomotion control system for quadruped and biped robots [5], [6], [84]. The locomotion control system receives commands related to the locomotion speed and gait pattern and creates motor torques through the RG and PF models to manipulate the robot. The RG model produces the rhythm information for locomotor behavior using phase oscillators and regulates the rhythm information by phase resetting in response to touch sensor signals. The PF model generates motor torques based on the rhythm information from the RG model to produce the joint movements.

B. Rhythm generator (RG) model

The RG model produces rhythm information for the locomotor behavior through interactions of the robot mechanical system, the oscillator network system, and the environment. For the RG model, we used six simple phase oscillators (Leg 1, Leg 2, Arm 1, Arm 2, Trunk, and Inter oscillators), which produce the basic rhythm for locomotion based on commands related to the locomotion speed and also receive touch sensor signals to modulate the rhythm by phase resetting (Fig. 3**B**).

Since the output from the α-motoneuron in the spinal cord controls the corresponding muscles, each joint may be controlled by separate neural oscillators. However, the oscillators must be coupled to coordinate interlimb movements [49]. For the locomotion control systems applying oscillators based on the concept of the CPG, the oscillators are classified into three main uses: 1. the use of an oscillator for the whole body [7–9], [56], [57], [87]; 2. the use of an oscillator for each limb [4–6], [10], [44]; and 3. the use of an oscillator for each joint [55], [78–80]. When we use an oscillator

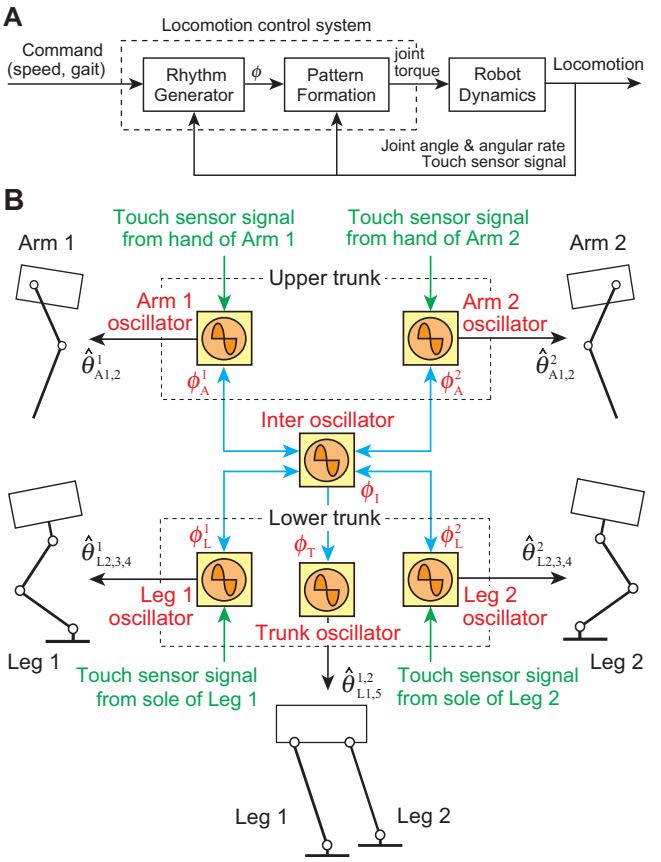

Fig. 3. Locomotion control system. **A** shows the two-layer hierarchical network model composed of the rhythm generator (RG) and pattern formation (PF) models. **B** shows the phase oscillators for producing locomotor rhythm and motor commands. The blue arrows indicate interactions among the oscillators based on the interlimb coordination pattern. The oscillator phases are modulated by phase resetting based on touch sensor signals (green arrows). The oscillator phases determine the limb kinematics (black arrows).

for each limb, the oscillators can manipulate the interlimb coordination pattern. When we use an oscillator for each joint, the oscillators can control the intralimb (intersegmental) coordination pattern, as well as the interlimb coordination pattern. In this paper, we focus on the control of the interlimb coordination pattern by the oscillators and use an oscillator for each limb, as explained in Section III-D.

We define $\phi^i_{\rm L}$, $\phi^i_{\rm A}$, $\phi_{\rm T}$, and $\phi_{\rm I}$ ($i = 1, 2$) as the phases of Leg i, Arm i, Trunk, and Inter oscillators, respectively, and employ the following phase dynamics:

$$\begin{aligned}
\dot{\phi}_{\rm I} &= \omega + g_{1\rm I} \\
\dot{\phi}_{\rm T} &= \omega + g_{1\rm T} \\
\dot{\phi}^i_{\rm A} &= \omega + g^i_{1\rm A} + g^i_{2\rm A} \quad i = 1, 2 \\
\dot{\phi}^i_{\rm L} &= \omega + g^i_{1\rm L} + g^i_{2\rm L} \quad i = 1, 2
\end{aligned} \tag{1}$$

where ω is the basic oscillator frequency that uses the same value for all the oscillators; $g_{1\rm I}$, $g_{1\rm T}$, $g^i_{1\rm A}$, and $g^i_{1\rm L}$ ($i = 1, 2$) are functions related to the interlimb coordination (see Section III-D); and $g^i_{2\rm A}$ and $g^i_{2\rm L}$ ($i = 1, 2$) are functions related to the phase and rhythm modulation and are based on the phase resetting in response to the touch sensor signals (see Section III-E).

C. Pattern formation (PF) model

Recent neurophysiological studies have revealed that spinocerebellar neurons receive sensory signals from proprioceptors and cutaneous receptors and encode the global information of the limb kinematics, such as the length and orientation of the limb axis [13], [63], [64]. In our control system, we used the PF model to determine the desired limb kinematics based on the oscillator phases and to produce motor torques for establishing the desired kinematics.

Locomotion in humans and animals involves moving the center of mass (COM) forward. To achieve this, they move the swing limb forward. When the swing limb touches the ground, it supports the body and generates a propulsive force from the ground. For simplicity, we used limb kinematics consisting of the swing and stance phases in the pitch plane (Fig. 4). For the leg motion, Joint 4 (ankle pitch joint) follows a simple closed curve relative to the trunk during the swing phase, which includes an anterior extreme position (AEP) and a posterior extreme position (PEP). Joint 4 starts from PEP and continues until the foot touches the ground. During the stance phase, Joint 4 traces out a straight line from the landing position (LP) to PEP. During this phase, the foot moves in the opposite direction to the trunk. The trunk travels in the walking direction while the foot is in contact with the ground. In both the swing and stance phases, the angular movement of Joint 4 is designed so that the foot is parallel to the line that connects points AEP and PEP.

For the leg movement, we use D to denote the distance between AEP and PEP. We define the swing and stance phase durations as $T_{\rm sw}$ and $T_{\rm st}$, respectively, for the case that the foot touches the ground at AEP (LP = AEP). The duty factor β (i.e., the ratio between the stance phase and the step cycle duration), the basic frequency ω in (1), the stride length S, and the locomotion speed v are then given by

$$\beta = \frac{T_{\rm st}}{T_{\rm sw}+T_{\rm st}},\ \omega = \frac{2\pi}{T_{\rm sw}+T_{\rm st}},\ S = \frac{T_{\rm sw}+T_{\rm st}}{T_{\rm st}}D,\ v = \frac{D}{T_{\rm st}} \tag{2}$$

These values are satisfied regardless of the gait pattern.

The lower trunk is at an angle of $\psi_{\rm H}$ to the line perpendicular to the line connecting points AEP and PEP. The height and forward bias from the center of points AEP and PEP to Joint 2 (hip pitch joint) are defined as parameters $\Delta_{\rm L}$ and $H_{\rm L}$, respectively. These trajectories for the legs provide the desired motion $\hat{\theta}^i_{{\rm L}j}$ $(i = 1, 2,\ j = 2, 3, 4)$ of Joint j (hip, knee, and ankle pitch joints) of Leg i by the function of phase $\phi^i_{\rm L}$ of Leg i oscillator, where we use $\phi^i_{\rm L} = 0$ at point PEP and $\phi^i_{\rm L} = \phi_{\rm AEP} (= 2\pi(1-\beta))$ at point AEP.

To increase the stability of bipedal locomotion in three-dimensional space, we used roll joints in the legs. We designed the desired motions $\hat{\theta}^i_{\rm L1}$ and $\hat{\theta}^i_{\rm L5}$ $(i = 1, 2)$ of Joints 1 and 5 (hip and ankle roll joints) of Leg i by the functions of phase $\phi_{\rm T}$ of Trunk oscillator by

$$\begin{aligned} \hat{\theta}^i_{\rm L1} &= R\cos(\phi_{\rm T}+\delta) \\ \hat{\theta}^i_{\rm L5} &= -R\cos(\phi_{\rm T}+\delta) \end{aligned} \tag{3}$$

where R is the amplitude of the roll motion and δ determines the phase relationship between the leg movements in the pitch and roll planes.

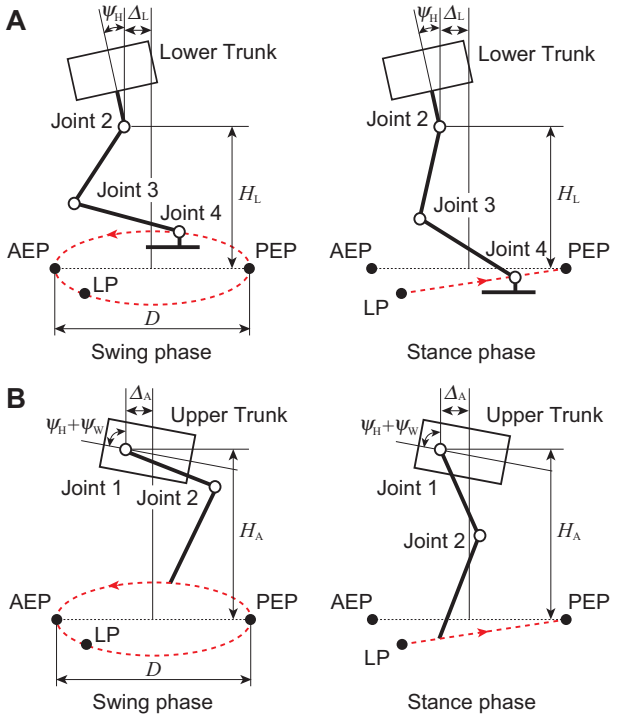

Fig. 4. Desired limb kinematics composed of swing and stance phases. **A** and **B** show the desired trajectories for the feet and the hands, respectively. When the foot or the hand lands on the ground, the trajectory changes from the swing to the stance phase. When the foot or the hand reaches point PEP, the trajectory moves into the swing phase.

For the arm motion, the tip of the hand follows a simple closed curve during the swing phase and a straight line during the stance phase, as is similar to the leg motion except for the bend direction between Joint 2 of the arm (elbow pitch joint) and Joint 3 of the leg (knee pitch joint) (Fig. 4**B**). The upper trunk is at an angle of $\psi_{\rm H} + \psi_{\rm W}$ to the line perpendicular to the line that connects points AEP and PEP, where angle $\psi_{\rm W}$ is the pitch angle of Waist joint. The height and forward bias from the center of points AEP and PEP to Joint 1 (shoulder pitch joint) of the arm are defined as parameters $\Delta_{\rm A}$ and $H_{\rm A}$, respectively. For the distance D, the swing phase duration $T_{\rm sw}$, and the stance phase duration $T_{\rm st}$, we used the same values as those used for the legs. These trajectories for the arms give the desired motion $\hat{\theta}^i_{{\rm A}j}$ $(i, j = 1, 2)$ of Joint j (shoulder and elbow pitch joints) of Arm i by the function of phase $\phi^i_{\rm A}$ of Arm i oscillator, where we used $\phi^i_{\rm A} = 0$ at point PEP and $\phi^i_{\rm A} = \phi_{\rm AEP} (= 2\pi(1-\beta))$ at point AEP.

We used these desired limb kinematics for both gait patterns and changed parameters $\Delta_{\rm L}$, $\Delta_{\rm A}$, $H_{\rm L}$, $H_{\rm A}$, $\psi_{\rm H}$, $\psi_{\rm W}$, and R depending on the gait pattern (see Section IV). To achieve the desired joint motions, the PF model produces motor torques based on PD feedback control using high-gain feedback gains.

D. Interlimb coordination

For the generation of locomotion, interlimb coordination is essential [4], [10], [16], [75]. Quadrupeds change their interlimb coordination pattern, such as walk, trot, and gallop

patterns, depending on the situation [10]. However, for human bipedal walking, both legs generally move out of phase to prevent toppling over, both arms also move out of phase, and one arm and the contralateral leg move in phase, except for a walk in special situations, such as a curved walk [18] and a splitbelt treadmill walk [53], [65]. We employ this interlimb coordination pattern for both quadrupedal and bipedal locomotion. That is, we use the trot pattern for quadrupedal locomotion.

Since the desired limb kinematics are designed by the corresponding oscillator phases, the interlimb coordination pattern of our robot is given by the phase relationship, that is, the phase difference, between the oscillators. Therefore, functions $g_{1\mathrm{I}}$, $g_{1\mathrm{T}}$, $g^i_{1\mathrm{A}}$, and $g^i_{1\mathrm{L}}$ in (1) are given as follows by using the phase differences between the oscillators based on Inter oscillator,

$$\begin{aligned} g_{1\mathrm{I}} &= -\sum_{i=1}^{2} K_{\mathrm{A}} \sin(\phi_{\mathrm{I}} - \phi^i_{\mathrm{A}} - (-1)^i \pi/2) \\ &\quad -\sum_{i=1}^{2} K_{\mathrm{L}} \sin(\phi_{\mathrm{I}} - \phi^i_{\mathrm{L}} + (-1)^i \pi/2) \\ g_{1\mathrm{T}} &= -K_{\mathrm{T}} \sin(\phi_{\mathrm{T}} - \phi_{\mathrm{I}}) \\ g^i_{1\mathrm{A}} &= -K_{\mathrm{A}} \sin(\phi^i_{\mathrm{A}} - \phi_{\mathrm{I}} + (-1)^i \pi/2) \quad i = 1, 2 \\ g^i_{1\mathrm{L}} &= -K_{\mathrm{L}} \sin(\phi^i_{\mathrm{L}} - \phi_{\mathrm{I}} - (-1)^i \pi/2) \quad i = 1, 2 \end{aligned} \tag{4}$$

where the desired phase relations are given by the desired interlimb coordination pattern: $\phi^1_{\mathrm{A}} - \phi^2_{\mathrm{A}} = \pi$, $\phi^1_{\mathrm{L}} - \phi^2_{\mathrm{L}} = \pi$, and $\phi^1_{\mathrm{A}} - \phi^2_{\mathrm{L}} = 0$ ($\phi^2_{\mathrm{A}} - \phi^1_{\mathrm{L}} = 0$), and K_{L}, K_{A}, and K_{T} are gain constants. These interactions are shown by the blue arrows in Fig. 3**B**.

E. Phase resetting

Locomotion is well-organized motion generated through the dynamic interactions of the body, the nervous system, and the environment. The adequate integration of sensory signals in issuing motor commands is crucial for adaptive locomotor behaviors. Phase resetting contributes to the resetting of the locomotor rhythm induced by a shift in the phase based on sensory information [4].

In this paper, we investigated the functional roles of such rhythm and phase modulations by phase resetting based on the touch sensor signals during the gait transition. We incorporated the phase resetting mechanism by using functions $g^i_{2\mathrm{A}}$ and $g^i_{2\mathrm{L}}$ in (1). Specifically, when the hand of Arm i (the foot of Leg i) lands on the ground, phase ϕ^i_{A} of Arm i oscillator (phase ϕ^i_{L} of Leg i oscillator) is reset to ϕ_{AEP} from ϕ^i_{Aland} (ϕ^i_{Lland}) at the landing ($i = 1, 2$). Therefore, functions $g^i_{2\mathrm{A}}$ and $g^i_{2\mathrm{L}}$ are expressed as

$$\begin{aligned} g^i_{2\mathrm{A}} &= (\phi_{\mathrm{AEP}} - \phi^i_{\mathrm{Aland}})\delta(t - t^i_{\mathrm{Aland}}) \quad i = 1, 2 \\ g^i_{2\mathrm{L}} &= (\phi_{\mathrm{AEP}} - \phi^i_{\mathrm{Lland}})\delta(t - t^i_{\mathrm{Lland}}) \quad i = 1, 2 \end{aligned} \tag{5}$$

where t^i_{Aland} (t^i_{Lland}) is the time when the hand of Arm i (the foot of Leg i) lands on the ground ($i = 1, 2$) and $\delta(\cdot)$ denotes Dirac's delta function. Note that the touch sensor signals not only modulate the locomotor rhythm and its phase but also switch the arm and leg motions from the swing to the stance phase, as described in Section III-C.

The phase resetting mechanism by (5) has been used for various biped robots [5], [6], [55–57], where the usefulness for increasing the robustness against perturbations and sudden environmental changes has been demonstrated. In addition, we have analytically shown the contribution of phase resetting to the improvement of robustness based on a stability analysis using simple physical models, such as a compass model and a five-link planar model [7–9].

F. Parameter determination for locomotion control

This locomotion control system has the following parameters: D, T_{sw}, and T_{st} to determine the locomotion speed (2); Δ_{L}, Δ_{A}, H_{L}, H_{A}, ψ_{H}, ψ_{W}, and R to determine limb kinematics (Fig. 4); δ to determine the phase relationship between the leg movements in the pitch and roll planes (3); and K_{T}, K_{A}, and K_{L} for the interactions among the oscillators (4). We have to determine these parameters to establish stable locomotion, especially for bipedal locomotion. In particular, the synchronization of the roll and pitch motions during locomotion is crucial. Therefore, when D, T_{sw} T_{st}, Δ_{L}, Δ_{A}, H_{L}, and, H_{A} were chosen, we used R and δ for the roll motion and ψ_{W} or ψ_{H} for the pitch motion as tuning parameters [5]. In addition, we used large values for K_{T}, K_{A}, and K_{L} so that the movements of the right and left limbs remain out of phase to prevent a decrease in stability [4]. Note that this paper does not focus on the optimality of these parameters, but the emergence of adaptive functions during locomotion through interactions of the robot mechanical system, the oscillator network system, and the environment.

IV. Gait transition

A. Robot kinematics for each gait pattern

Based on the desired limb kinematics in Fig. 4, we illustrated the desired robot kinematics for quadrupedal and bipedal locomotion in Fig. 5, where COM indicates the center of mass of the upper trunk, l_{U} ($= 8.0$ cm) and l_{L} ($= 7.0$ cm) are the lengths from COM to Joint 1 of the arm (shoulder pitch joint) and Waist Joint in the pitch plane, respectively, l_{W} ($= 7.0$ cm) is the length from Waist Joint to Joint 1 of the leg (hip pitch joint), L_{A} and L_{L} are the forward biases from COM to the centers of the desired foot and hand trajectories, respectively, and $()^{\mathrm{Q}}$ and $()^{\mathrm{B}}$ indicate the parameters for quadrupedal and bipedal walking, respectively. Note that parameters L_{A} and L_{L} are determined by parameters Δ_{A}, Δ_{L}, ψ_{H}, and ψ_{W}, as follows:

$$\begin{aligned} L_{\mathrm{A}} &= l_{\mathrm{U}} \sin(\psi_{\mathrm{H}} + \psi_{\mathrm{W}}) + \Delta_{\mathrm{A}} \\ L_{\mathrm{L}} &= l_{\mathrm{L}} \sin(\psi_{\mathrm{H}} + \psi_{\mathrm{W}}) + l_{\mathrm{W}} \sin\psi_{\mathrm{H}} + \Delta_{\mathrm{L}} \end{aligned} \tag{6}$$

Also, note that $L^{\mathrm{B}}_{\mathrm{A}}$ and $L^{\mathrm{B}}_{\mathrm{L}}$ are both set to 0, as shown in Fig. 5**B**. Since the hands do not touch the ground during bipedal walking, the tip of the hand follows the closed curve.

In our control system, the gait pattern is determined by kinematic parameters Δ_{A}, Δ_{L}, H_{A}, H_{L}, ψ_{H}, and ψ_{W} for the pitch motion and kinematic parameter R that constructs the robot motions in the roll plane for bipedal locomotion.

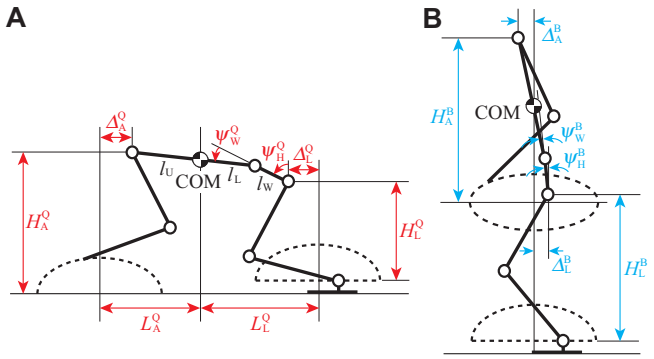

Fig. 5. Schematic diagrams and kinematic parameters for quadrupedal (**A**) and bipedal (**B**) walking

B. Gait transition strategy based on the physiological concept of synergy

To change the gait pattern, robot motions must connect one pattern to another. However, thousands of methods can create such robot motions, due to the redundancy of the degrees of freedom of the robot. Since our control system designed robot motions for quadrupedal and bipedal locomotion by using the same kinematic parameters, robot motions during the transition can be generated by changing these parameters from $\Delta_{\mathrm{A}}^{\mathrm{Q}}$, $\Delta_{\mathrm{L}}^{\mathrm{Q}}$, $H_{\mathrm{A}}^{\mathrm{Q}}$, $H_{\mathrm{L}}^{\mathrm{Q}}$, $\psi_{\mathrm{T}}^{\mathrm{Q}}$, and R^{Q} to $\Delta_{\mathrm{A}}^{\mathrm{B}}$, $\Delta_{\mathrm{L}}^{\mathrm{B}}$, $H_{\mathrm{A}}^{\mathrm{B}}$, $H_{\mathrm{L}}^{\mathrm{B}}$, $\psi_{\mathrm{T}}^{\mathrm{B}}$, and R^{B}. However, we still have many parameters. We must determine how to change them and solve this redundancy problem, which is a crucial issue.

Physiological findings suggest the importance of muscle synergies for controlling movements in humans and animals [20–22], [24], [25], [43], [82], [83]; these concepts have been analyzed using principal component analysis and factor analysis and are viewed as one solution to handle the redundancy problem in biological systems. Muscle synergy is related to the co-variation of muscle activities. Ivanenko *et al.* [41], [42] reported that, although recorded electromyographic data during human bipedal locomotion are complicated, the data can be accounted for by a combination of only five basic patterns. Furthermore, similar movement patterns such as obstacle avoidance and kick motion share the same basic patterns and can be explained by adding another basic pattern.

In addition to muscle synergies, kinematic synergies have been investigated during human whole-body movements [1–3], [28], [30]. Most studies have associated kinematic synergies with simultaneous movements in several joints. Freitas *et al.* [28] investigated joint angle co-variation patterns during a rhythmic whole-body motion and suggested that two kinematic synergies account for the joint co-variation and contribute to the stabilization of two performance variables, the COM location and the trunk orientation. This means that some degrees of freedom are functionally connected by objects, depending on the task, which reduces the number of degrees of freedom and solves the problem of motor redundancy. Such angle co-variation behavior is also observed during the locomotion of humans and animals [12], [30], [45], [64]. When elevation angles at the thigh, shank, and foot during locomotion are plotted, one versus the others, the angles describe regular loops constrained on a plane [12], [45], [64], and hint that such a kinematically coordinative structure is embedded in the motion generation mechanism.

In this paper, using these physiological findings, we produced robot motions during gait transition by constructing coordinative structures. To change the gait pattern from quadrupedal to bipedal locomotion, the robot raises its trunk and its arms leave the ground. Since the number of limbs that support the body is reduced, an adequate location between the supporting limb locations and the COM location is crucial when raising the trunk; otherwise, the robot easily falls over. In addition, since raising the trunk induces a large change in the robot posture and the COM location, the appropriate change in trunk orientation is crucial. Therefore, to control the COM location relative to the supporting positions of the limbs and the trunk orientation, similarly to [28], we used two performance variables and constructed a kinematically coordinative structure, as shown in the next section.

C. Kinematic coordination during gait transition

To handle the redundancy problem in the motion planning for gait transition, we employed two performance variables, ξ_1 and ξ_2, that control the horizontal positions of the arms and feet relative to the COM and the trunk orientation, respectively, and produce robot motions by constructing a kinematically coordinative structure using these two performance variables. In particular, we encoded seven kinematic parameters: Δ_{A}, Δ_{L}, H_{A}, H_{L}, ψ_{H}, ψ_{W}, and R using performance variables ξ_1 and ξ_2 (Fig. 6) by

$$
\begin{aligned}
\Delta_{\mathrm{A}}(\xi_1,\xi_2) &= \Delta_{\mathrm{A}}^{\mathrm{Q}} - \{l_{\mathrm{U}}\sin(\psi_{\mathrm{H}}(\xi_1,\xi_2)+\psi_{\mathrm{W}}(\xi_1,\xi_2)) + \Delta_{\mathrm{A}}^{\mathrm{Q}}\}\xi_1 \\
\Delta_{\mathrm{L}}(\xi_1,\xi_2) &= \Delta_{\mathrm{L}}^{\mathrm{Q}} - \{l_{\mathrm{L}}\sin(\psi_{\mathrm{H}}(\xi_1,\xi_2)+\psi_{\mathrm{W}}(\xi_1,\xi_2)) \\
&\qquad + l_{\mathrm{W}}\sin\psi_{\mathrm{H}}(\xi_1,\xi_2) + \Delta_{\mathrm{L}}^{\mathrm{Q}}\}\xi_1 \\
H_{\mathrm{A}}(\xi_1,\xi_2) &= H_{\mathrm{A}}^{\mathrm{Q}} + (H_{\mathrm{A}}^{\mathrm{B}} - H_{\mathrm{A}}^{\mathrm{Q}})\xi_2 \\
H_{\mathrm{L}}(\xi_1,\xi_2) &= H_{\mathrm{L}}^{\mathrm{Q}} + (H_{\mathrm{L}}^{\mathrm{B}} - H_{\mathrm{L}}^{\mathrm{Q}})\xi_2 \\
\psi_{\mathrm{H}}(\xi_1,\xi_2) &= \psi_{\mathrm{H}}^{\mathrm{Q}} + (\psi_{\mathrm{H}}^{\mathrm{B}} - \psi_{\mathrm{H}}^{\mathrm{Q}})\xi_2 \\
\psi_{\mathrm{W}}(\xi_1,\xi_2) &= \psi_{\mathrm{W}}^{\mathrm{Q}} + (\psi_{\mathrm{W}}^{\mathrm{B}} - \psi_{\mathrm{W}}^{\mathrm{Q}})\xi_2 \\
R(\xi_1,\xi_2) &= R^{\mathrm{Q}} + (R^{\mathrm{B}} - R^{\mathrm{Q}})(1 - e^{-\kappa\xi_2})
\end{aligned}
\tag{7}
$$

These functions mean that performance variables ξ_1 and ξ_2 are used to horizontally move the foot and hand trajectories closer to the COM and to raise the trunk, respectively. By using this controller, gait transition is achieved by simply changing the performance variables (ξ_1, ξ_2) from (0, 0) to (1, 1), as shown in Fig. 7. Since the roll motion is crucial during bipedal locomotion, we determined kinematic parameter R by using an exponential function of performance variable ξ_2, where κ is a parameter.

To prepare adequate kinematic coordination during the transition, we designed the change of performance variables ξ_1 and ξ_2 by the following two steps (Fig. 8):

Step 1: When the control system receives a command to change the gait pattern, it increases performance variable ξ_1 from 0 to $\bar{\xi}_1$ ($0 \le \bar{\xi}_1 \le 1$) during time interval T_1.

Step 2: After Step 1 and when phase ϕ_{I} of Inter oscillator is at ϕ_{raise}, performance variables ξ_1 and ξ_2 are increased

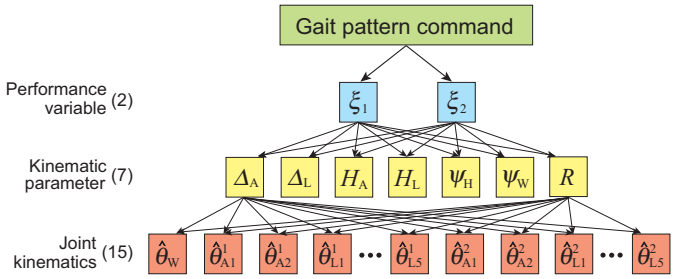

Fig. 6. Motion planning of joint kinematics using two performance variables derived from the kinematic parameters

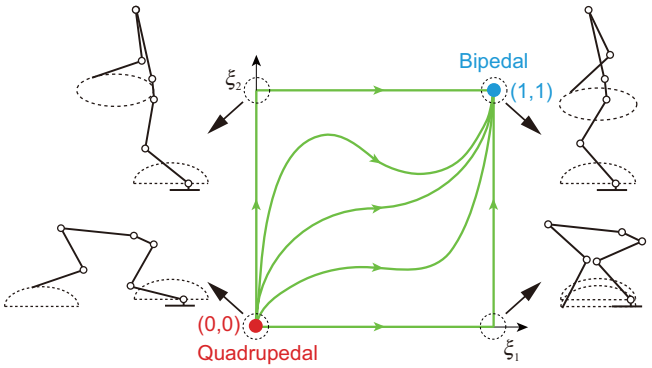

Fig. 7. Trajectories in the ξ_1-ξ_2 plane for gait transition from quadrupedal to bipedal. The roles of ξ_1 and ξ_2 enable hand and foot trajectories to be closer to the COM and raise the trunk, respectively.

from $\bar{\xi}_1$ to 1 and from 0 to 1, respectively, during time interval T_2.

This strategy moves the foot and hand trajectories closer to the COM during Step 1 while it walks quadrupedally. During Step 2, the robot raises its trunk to start walking bipedally.

D. Parameter determination for gait transition

For gait transition control, we have to determine the following parameters: κ to determine how quickly to produce the roll motion for bipedal locomotion; $\bar{\xi}_1$ to determine the relationship between the foot and hand trajectories and the COM; ϕ_{raise} to determine the timing to start Step 2; and T_1 and T_2 to determine the durations for Steps 1 and 2. In particular, we used a large value for κ because the roll motion is important during bipedal locomotion. Since the timing and speed to raise the trunk are crucial to establish the gait transition, T_2 and ϕ_{raise} are especially important among these parameters in this parameter determination. Therefore, we investigated the roles of these two parameters in gait transition (see Section V-E).

V. Results

A. Quadrupedal and bipedal locomotion

In this section, we verify that our control system establishes stable quadrupedal and bipedal locomotion based on numerical simulations and experiments, and that the numerical simulations and experiments show similar dynamics by comparing the results. We used the following parameters: $D = 3.0$ cm, $T_{\text{sw}} = 0.35$ s, $T_{\text{st}} = 0.35$ s, $\delta = -150°$, $K_{\text{T}} = 10.0$, $K_{\text{A}} = 2.0$, and $K_{\text{L}} = 2.0$; the remaining parameters are shown in Table II.

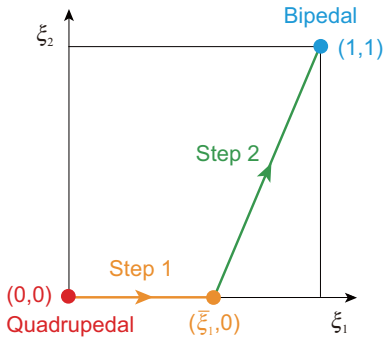

Fig. 8. Designed trajectory in the ξ_1-ξ_2 plane to change the gait pattern from quadrupedal to bipedal

TABLE II
KINEMATIC PARAMETERS FOR QUADRUPEDAL AND BIPEDAL LOCOMOTION

Parameter	Quadrupedal	Bipedal
Δ_{A} [cm]	0	0.7
Δ_{L} [cm]	0	-2.4
H_{A} [cm]	19	18
H_{L} [cm]	14	15
ψ_{H} [deg]	31.4	0
ψ_{W} [deg]	64.7	5.0
R [deg]	0	4.0

These parameter settings result in $\beta = 0.5$, $S = 6.0$ cm, $v = 0.86$ cms^{-1} in (2).

Figures 9 and 10 compare the results between the numerical simulations and the experiments for quadrupedal and bipedal locomotion, respectively. **A** and **B** are snapshots for the numerical simulations and the experiments, respectively (see supplementary movies). **C** shows the angular rate profiles for the roll and pitch motions of the trunk relative to the ground. The experimental results are monitored by the gyro sensors and are filtered with a low-pass cutoff of 20 Hz to eliminate noise. **D** is the phase diagram for the roll and pitch behaviors. Except for the roll motion during bipedal locomotion, the desired joint motions are designed to avoid influencing the trunk movements relative to the ground. The resultant behaviors of the trunk show the dynamic influences between the robot movements and the environment. Although the movements in the experimental results are larger than the simulation results due to various uncertainties such as backlash, they differ in a consistent manner during each cycle and the shapes of the profiles in the numerical simulations and the experiments look similar. The roll and pitch motions continue periodic movements, verifying that the robot achieves stable quadrupedal and bipedal locomotion.

B. Gait transition

In this section, we demonstrate by numerical simulations and experiments that our control system attains gait transition from quadrupedal to bipedal locomotion. For the gait transition, we used the following parameters: $\kappa = 6.0$, $\bar{\xi}_1 = 0.7$, $\phi_{\text{raise}} = 0.83\pi$, $T_1 = 5.0$ s, and $T_2 = 2.0$ s.

Figure 11 compares the results between the numerical simulations and the experiments for the gait transition from quadrupedal to bipedal locomotion. **A** and **B** display snapshots

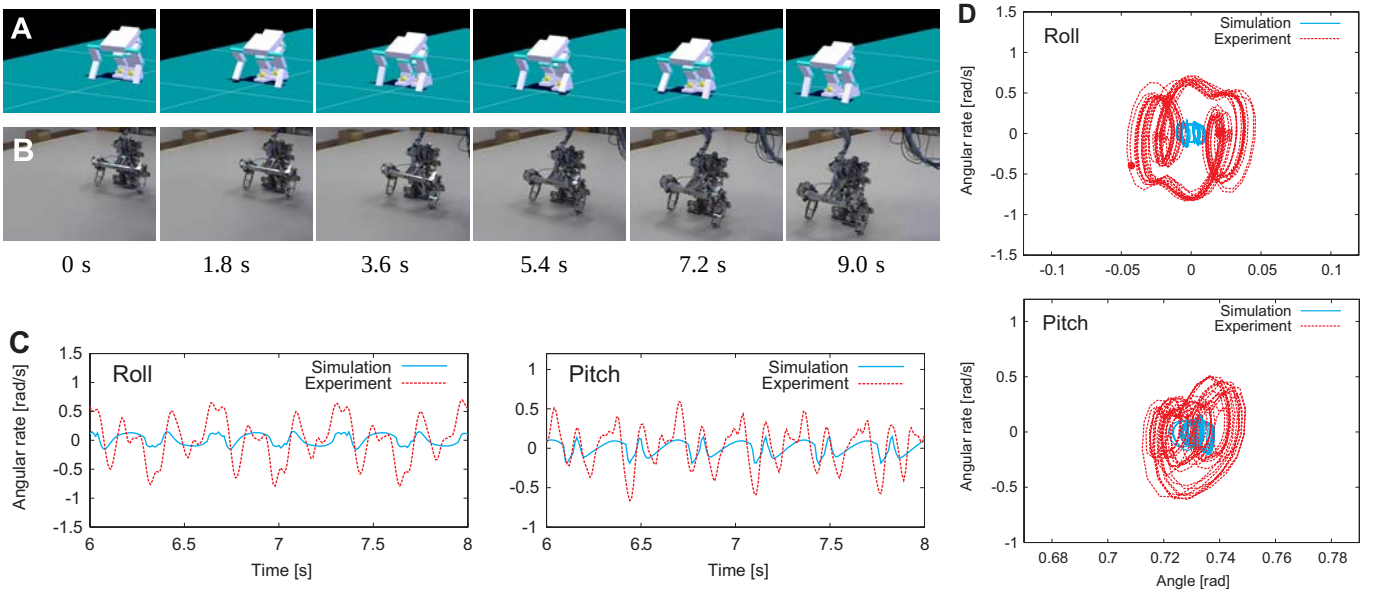

Fig. 9. Quadrupedal locomotion. Snapshots for the numerical simulation (**A**) and the experiment (**B**) (see supplementary movies). Time stamps correspond to both the numerical simulation and the experiment. Angular rate profiles (**C**) and phase diagrams (**D**) for the roll and pitch motions. The black dots indicate initial states.

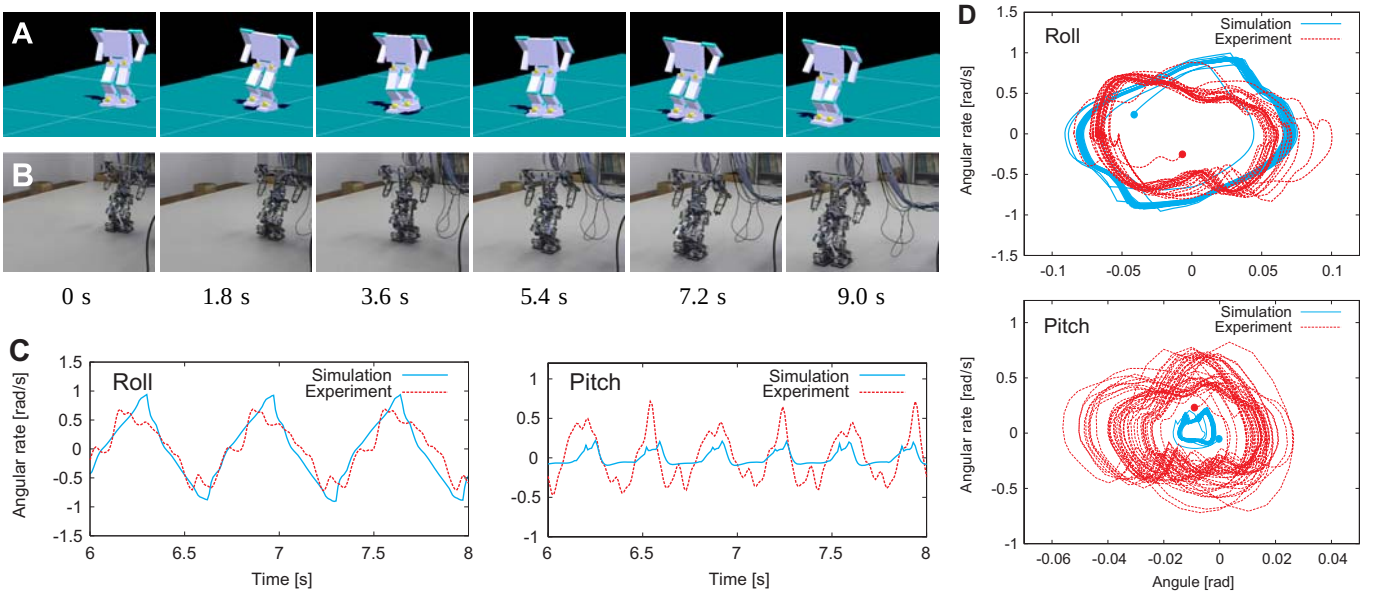

Fig. 10. Bipedal locomotion. Snapshots for the numerical simulation (**A**) and the experiment (**B**) (see supplementary movies). Time stamps correspond to both the numerical simulation and the experiment. Angular rate profiles (**C**) and phase diagrams (**D**) for the roll and pitch motions. The black dots indicate initial states.

for the numerical simulations and the experiments, respectively (see supplementary movies). **C** and **D** are the angular rate profiles and the phase diagrams, respectively, for the roll and pitch motions of the trunk. The roll and pitch motions show that they move from the periodic movement of quadrupedal locomotion to that of bipedal locomotion through Steps 1 and 2, therefore verifying that the robot establishes the gait transition from quadrupedal to bipedal locomotion.

C. Distance between the COM position and the support polygon

To show the dynamics of the established quadrupedal and bipedal locomotion and the gait transition, we used the numerical simulation to investigate the relationship between the positions of the COM of the whole body and the support polygon. We project the COM position to the ground and calculate the distance between the projected COM position and the closest line of the support polygon. When the COM is located inside the polygon, the distance is a negative value. When the COM is located outside the polygon, the distance is a positive value. That is, a positive distance indicates that the gait pattern is statically unstable and the robot achieves dynamically stable locomotion. In this calculation, when at least a part of the sole contacts the ground, we assumed that all of the sole contacts the ground. Since the support polygon is overestimated, even if the gait is estimated as statically

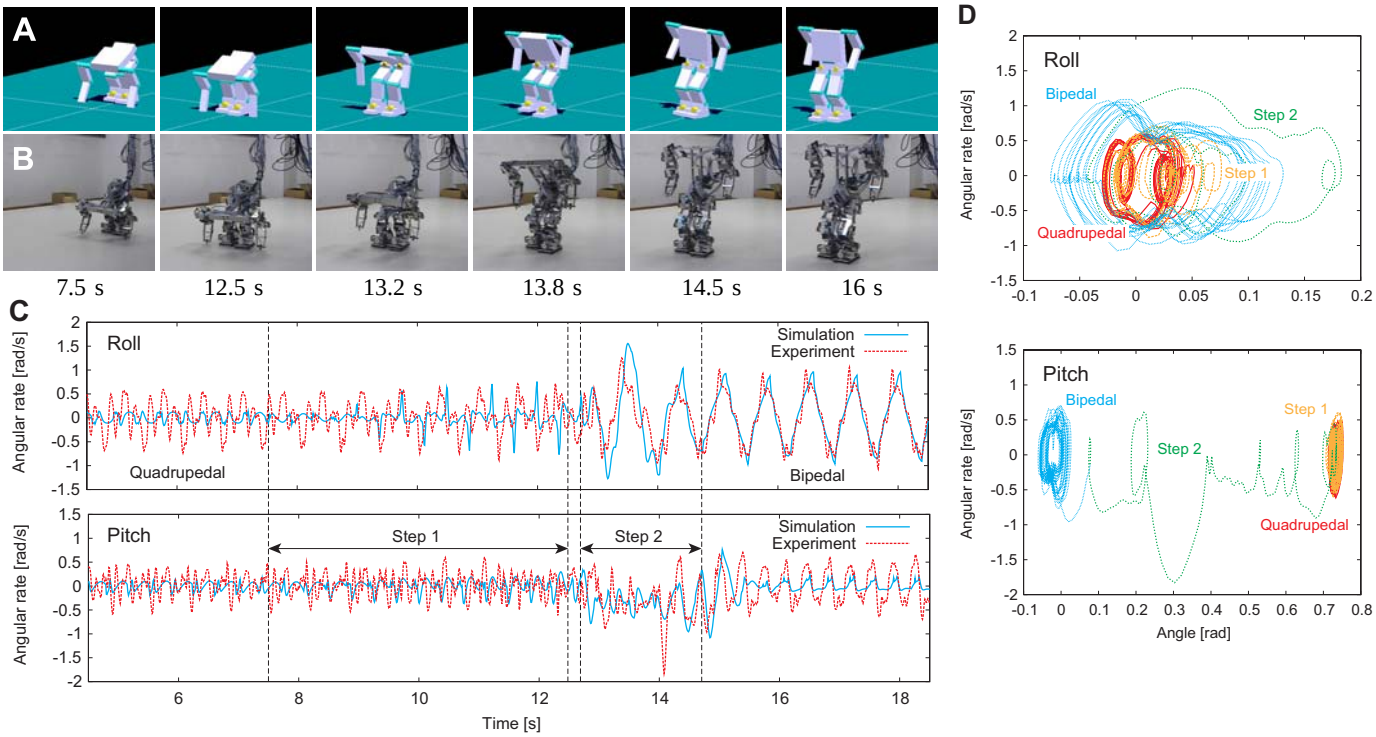

Fig. 11. Gait transition from quadrupedal to bipedal locomotion. Snapshots for the numerical simulation (**A**) and the experiment (**B**) (see supplementary movies). Time stamps correspond to both the numerical simulation and the experiment. Angular rate profiles (**C**) and phase diagrams (**D**) for the roll and pitch motions. **D** shows the experimental result.

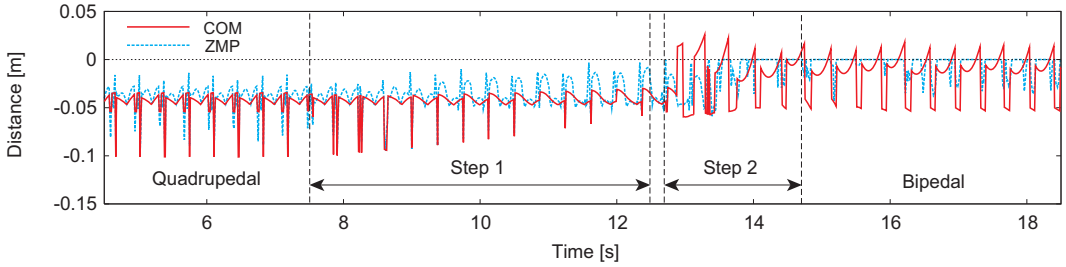

Fig. 12. Distances between the COM position and the support polygon and between the ZMP position and the support polygon during the gait transition from quadrupedal to bipedal locomotion. Negative values indicate the COM (ZMP) is inside the polygon. Positive values indicate the COM (ZMP) is outside the polygon. During Step 2 and bipedal locomotion, the distance for the COM is outside the polygon in some phases.

stable, the actual gait may be statically unstable. However, when the gait is estimated as statically unstable, the actual gait is statically unstable. In addition to the COM position, we also investigated the relationship between the positions of the zero moment point (ZMP) [34], [85] and the support polygon to show the dynamic properties. Here, a negative distance means that the ZMP is located inside the polygon.

Figure 12 shows the distances between the COM position and the support polygon and between the ZMP position and the support polygon for the gait transition established in the last section (Fig. 11). The ZMP position is inside the polygon during this gait transition, although the safety margin largely changes depending on the gait patterns and situations. The COM is inside the polygon during quadrupedal locomotion and Step 1 of the gait transition, which means these gait patterns are statically stable. However, from Step 2, in some phases the COM is outside the polygon despite the overestimation of the support polygon; this indicates that, at least during Step 2 and bipedal locomotion, the locomotor behaviors are statically unstable and the robot achieves dynamically stable locomotion.

D. Effects of phase and rhythm modulations by phase resetting

As shown in the previous section, at least from Step 2 in the gait transition, locomotor behavior is statically unstable and the robot establishes dynamically stable locomotion. In this section, we investigate the effects of phase and rhythm modulations by phase resetting for achieving such dynamically stable locomotion during the gait transition.

We carried out the numerical simulations and the experiments of gait transition without incorporating phase resetting, without which the phase and rhythm are not modulated and the swing and stance phases of the desired leg and arm trajectories change at points AEP and PEP (Fig. 4) independently of the touch sensor signals. We examined whether the robot achieves the gait transition by applying the same parameters

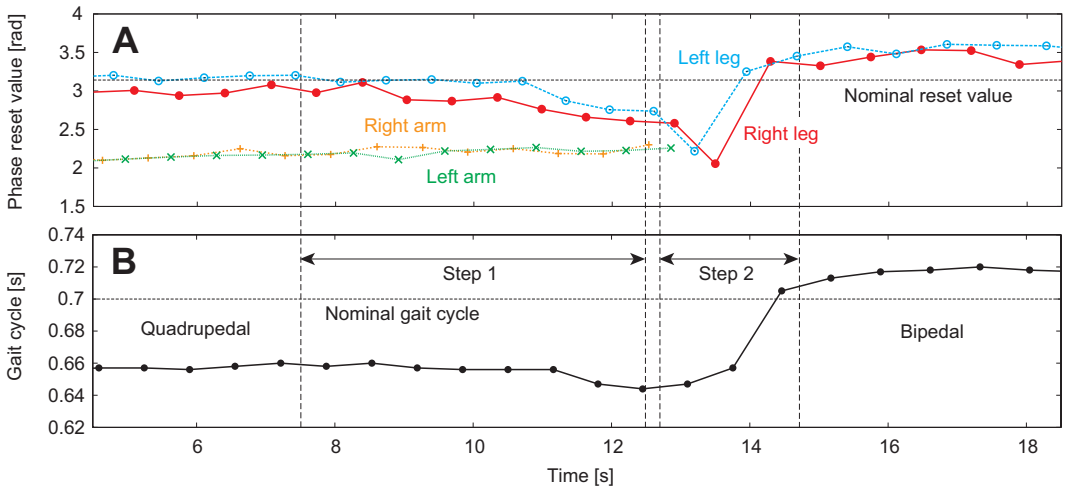

Fig. 14. Modulation of the locomotion phase and rhythm by phase resetting during the gait transition. **A**: phase reset value and **B**: gait cycle.

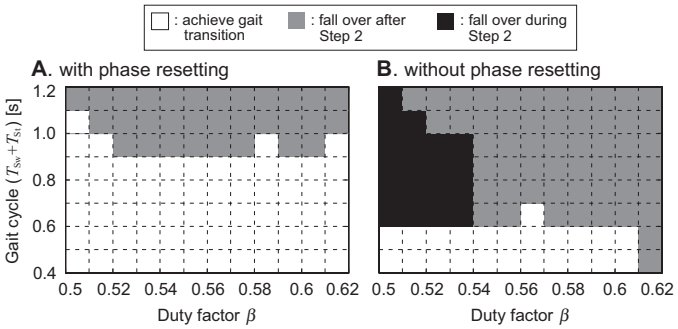

Fig. 13. Effects of gait cycle and duty factor on the success and failure of the gait transition with phase resetting (**A**) and without phase resetting (**B**). The lower left corner of each box (0.01×0.1 s) corresponds to the axis value.

used in the previous sections. However, the robot could not establish the gait transition and easily fell over. Then, we performed numerical simulations using various values of the gait cycle ($T_{\rm sw}+T_{\rm st}$) and duty factor β in (2) by manipulating the swing phase duration $T_{\rm sw}$ and the stance phase duration, $T_{\rm st}$ and investigated whether the robot establishes the gait transition. Figure 13 compares the results with and without phase resetting by examining whether the robot achieves the gait transition, falls over after Step 2, or falls over during Step 2. When we did not use phase resetting, the robot achieved the gait transition only for short gait cycles. The robot with phase resetting established the gait transition for more various gait cycles and duty factors than the robot without phase resetting. For the robot experiments, when we used the shortest possible gait cycle, the robot without phase resetting sometimes achieved the gait transition. However, the results were not robust. These results suggest that phase and rhythm modulations by phase resetting are a crucial factor for establishing dynamically stable locomotion during the gait transition.

To clarify the contribution of phase resetting for establishing a stable gait, we investigated the modulation of the locomotion phase and rhythm during the gait transition. Figure 14 shows the phase reset values and gait cycles obtained by the experiment in Fig. 11, where the gait cycle is calculated by Inter oscillator. The oscillator phases are reset based on the touch sensor signals and regulated depending on the situation, which results in modulation of the gait cycle durations. The arm oscillators are reset earlier than are the leg oscillators, and the phase reset of the arm oscillators does not occur after Step 2, because the robot starts bipedal locomotion. The reset values of the leg oscillators are different between the gait patterns, and significantly change during Step 2, because the locomotor behavior is disturbed due to the start of bipedal locomotion. These results suggest that phase resetting helps to increase the robustness in the gait transition.

To further clarify the functional roles of phase resetting in the gait transition, we performed numerical simulations to examine the contribution of phase resetting to adaptations to perturbations and various environments [4–6]. Regarding the adaptation to perturbations, we used various magnitudes of force perturbation in the walking direction or the opposite direction for 100 ms at the middle of Step 2 and investigated whether the robot establishes the gait transition. For the adaptation to various environments, we employed various slope angles and examined whether the robot achieves the gait transition. To compare the results with and without phase resetting, we used $T_{\rm sw} = 0.2\ s$ and $T_{\rm st} = 0.2\ s$, since the robot establishes the gait transition using these parameters, as investigated by the computer simulation shown in Fig. 13. Figure 15 shows the results, which illustrate that phase resetting contributes to the adaptations to perturbations and various environments in the gait transition.

E. Effects of the timing and the speed to change the gait pattern

As shown in the previous section, phase and rhythm modulation plays an important role in establishing stable gaits during the gait transition. Since drastic changes in the robot posture and the reduction of the number of supporting limbs during Step 2 in the gait transition greatly affect the stability, as shown in Section V-C, the timing and the speed of raising the trunk are also crucial factors. To investigate these effects, we changed parameters $\phi_{\rm raise}$ and T_2 and examined whether the

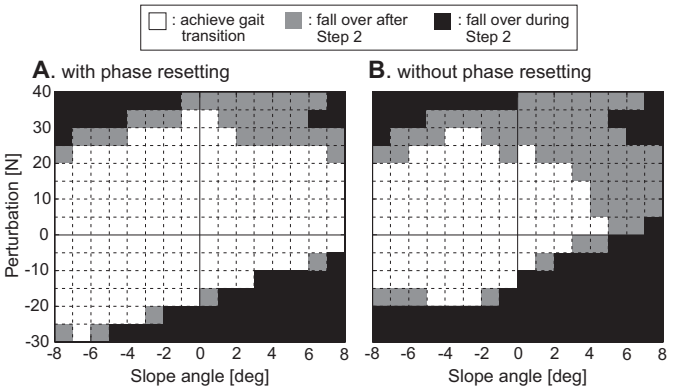

Fig. 15. Adaptations to force perturbations and slope angles with phase resetting (**A**) and without phase resetting (**B**). The lower left corner of each box (1 deg $\times$ 5 N) corresponds to the axis value. The positive perturbation means the perturbation is added in the walking direction. The positive slope means the upslope.

robot establishes the transition. Since the mechanical system of the robot is almost symmetric between the right and left sides, we employed $0 \leq \phi_{\text{raise}} < \pi$. For the numerical simulations, we examined whether the robot achieves the gait transition, falls over after Step 2, or falls over during Step 2. For the experiments, we carried out the gait transition experiment five times for each parameter set and calculated the success rate.

Figure 16 shows the results. The numerical simulations and the experiments obtain similar results. When the gait pattern changes slowly with large T_2, the robot easily establishes the gait transition. However, when the gait transition is conducted quickly with small T_2, the dynamic effects of the quick change of the gait pattern influence the success rate of the gait transition. The timing to start raising the trunk also affects the success rate. Figure 17 shows the footprint diagram for phase ϕ_{I} of Inter oscillator before Step 2 in the experiment. The comparison between Figs. 16 and 17 implies that for successful gait transition, the timing to start raising the trunk is when the robot is supported by one leg and one arm. In contrast, supporting the robot by both arms often leads to transition failure. These results suggest that these factors influence the dynamics that govern the gait transition from quadrupedal to bipedal locomotion.

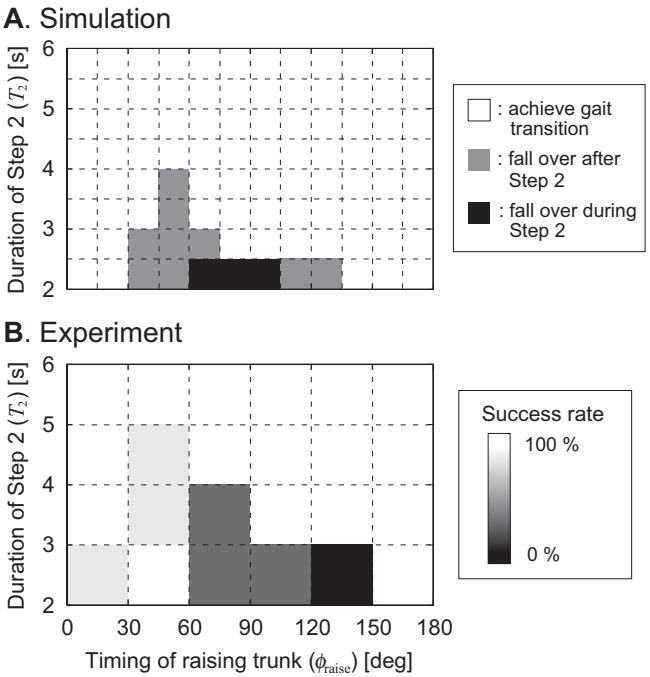

Fig. 16. Effects of timing and speed of raising the trunk on the success and failure of the gait transition for the numerical simulation (**A**) and the experiment (**B**). The lower left corner of each box (15 deg $\times$ 0.5 s for **A**, 30 deg $\times$ 1.0 s for **B**) corresponds to the axis value.

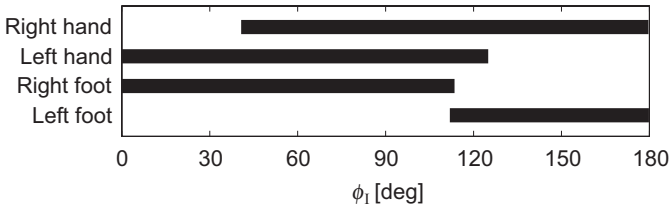

Fig. 17. Footprint diagram of the experimental result for phase ϕ_{I} of Inter oscillator before Step 2

VI. Discussion

A. Challenge of the gait transition task

Although many studies have investigated methods to achieve stable locomotor behaviors for various gait patterns of legged robots, their transitions have not been thoroughly examined. To establish the gait transition of a biped robot from quadrupedal to bipedal locomotion, robot motions must be created to produce stable quadrupedal and bipedal locomotion, and in addition, to connect the quadrupedal locomotion to the bipedal locomotion without the robot falling over due to the drastic changes in the robot posture and the reduction of the number of supporting limbs.

In this gait transition, the following two issues are crucial. (1) Since a robot has many degrees of freedom, it is difficult to determine how to produce robot motions to connect one gait pattern to another; in other words, how to construct adequate constraint conditions in motion planning. (2) Even if the robot establishes stable quadrupedal and bipedal locomotion, it may fall over during the gait transition and it is difficult to establish stable gait transition without falling over.

B. Handling of the redundancy problem

Regarding the first issue above, various approaches exist, for example, constructing an evaluation index and producing robot motions through optimization of the index or producing robot motions while satisfying the stability criteria of the ZMP [85]. Asa *et al.* [11] conducted a two-dimensional simulation of the gait transition of a biped robot between quadrupedal and bipedal locomotion by constructing a potential function to produce robot motions. In this paper, we applied the physiological concept of synergies to create the robot motions during the gait transition by constructing kinematically coordinative structures for the transition task and focusing on the COM location relative to the supporting positions of the limbs and the trunk orientation. These coordinative structures create adequate constraints for the degrees of freedom of the robot and solve the redundancy problem.

C. The roles of phase resetting

Regarding the second issue, we investigated the roles of phase resetting and demonstrated that phase resetting contributes to the generation of robust gait transition. The spatiotemporal patterns of torque commands determine the locomotor behavior, and phase resetting results in temporal modulation of this behavior based on the touch sensor signals. Even if the timing of ground contact events is disturbed depending on the gait pattern, perturbation, and environmental situation, phase resetting allows the generation of command signals based on such events. Early ground-contact events induce a phase shift of periodic command signals to interrupt the locomotor rhythm, as shown during Step 2 in the gait transition (Fig. 14). Delayed ground-contact events result in a phase shift of periodic command signals to prolong the locomotor rhythm, as shown during bipedal locomotion (Fig. 14). Phase resetting creates various phase profiles and locomotor rhythms that depend on the situation, and thus improves the robustness in the gait transition despite its simple mechanism, as shown in Figs. 13 and 15. These results are consistent with our simulation results of a biological system [4].

Locomotion of humans and animals is created based on movement control and posture control. Movement control produces periodic command signals to create periodic limb movements for forward motion. In contrast, posture control produces command signals based on somatosensory and vestibular information at the brainstem and cerebellar levels to control and regulate the postural behavior that prevents falling over. Phase resetting contributes to modulation of the timing to produce the movement control signals [4]. The command signals by the movement and posture controls are integrated at the spinal cord level. The movement and posture controls contribute to establishing dynamic locomotion. However, in this paper, we did not incorporate the posture control model in order to clearly investigate the roles of phase resetting in the modulation of periodic limb movements during the gait transition.

Although this paper focused on the gait transition from quadrupedal to bipedal locomotion, the gait transition from bipedal to quadrupedal locomotion should be also discussed. Our results show that quadrupedal locomotion is statically stable, although bipedal locomotion is statically unstable and dynamically stable (Fig. 12) (we investigated the dynamic stability using the COM and ZMP positions, but the relationship of the COM position and its velocity with the support polygon would also be useful [38]). This stability characteristic suggests that we can also achieve the gait transition from bipedal to quadrupedal by applying our gait transition strategy. However, we should note the following difference. As explained above, for the gait transition from quadrupedal to bipedal, the stability during raising the trunk is crucial. That is, the reduction of the number of supporting limbs and the change of the COM position of the whole body influence walking stability. In contrast, the gait transition from bipedal to quadrupedal moves the COM position forward to bring down the trunk during bipedal locomotion, which may induce the robot to fall down forward. This causes a large impact on the arms and destabilizes the walking. We confirmed that our strategy is also applicable to this gait transition by performing the robot experiment (see supplementary movie).

D. Timing and speed to change the gait pattern

Since the gait transition requires drastic changes in the robot posture and the reduction of the number of supporting limbs, the timing and speed of raising the trunk are also crucial factors to establish stable transition. When the gait patterns are statically stable, these factors have almost no influence. However, when the gait patterns are statically unstable and dynamically stable, as shown in Fig. 12, these factors greatly influence the success rate of the gait transition (Fig. 16). The phase-dependent stability characteristics are caused by a statically unstable gait during Step 2 and bipedal locomotion.

To create bipedal locomotion of a robot from the quadrupedal posture, we can create the robot motions to make the robot first stand up (the robot motion stops), and then to make it start bipedal locomotion, which is a different approach from that in this paper. However, humans and animals change their gait patterns without stopping their movements between walking and running, straight walking and turning, and quadrupedal and bipedal locomotion. This means that their periodic movements continuously change into another periodic movements. Such gait pattern transition for the robot is more difficult than the gait pattern transition in which the robot once stops before the transition, and we focused on the gait transition during walking without stopping the movements. The effects of timing and speed on changing the gait pattern (Fig. 16) clearly show this difficulty.

Humans and animals change their gait patterns smoothly or abruptly depending on the species and the situation [32], [47], [66], [69]. In this paper, we used various speeds to change the gait pattern using T_2 (Fig. 16). Since the Japanese macaque (*Macaca fuscata*) establishes the gait transition from quadrupedal to bipedal almost within one gait cycle [59], our speed appears to be slow ($T_2 > T_{\mathrm{sw}} + T_{\mathrm{st}}$). However, this speed greatly influences the stability during the gait transition. When we used a high speed for the gait transition (small T_2), the robot easily fell down. Since we focused on the investigation of the functional roles of phase resetting in the gait transition by using simple designs, we did not use any optimization in the motion planning for each gait pattern and the gait transition. For such an abrupt gait transition, we may need more precise motion planning by considering the conservation of momentum and ZMP criteria, as well as the COM location and the trunk orientation.

E. Control design inspired from biological systems

Recently, interest in the study of legged robots has increased. However, unlike humans and animals, these robots still have difficulties in achieving adaptive behaviors in various situations, and a huge gap remains between them. Therefore, to create new control strategies, it is natural to use ideas inspired from biological systems and many biologically-inspired robots have been developed. For example, computational approaches of motor learning by imitation have been used to create

various movements of humanoid robots [31], [72], [73]. The physiological concept of the CPG has been widely used in the locomotion control of legged robots [19], [27], [39], [40], [44], [55–57], [77]. We also have established adaptive locomotor behaviors of a biped robot to perturbations and sudden environmental changes, such as slopes [5], and produced adaptive turning behaviors [6]. In this paper, we improved our control systems based on the physiological findings and achieved the gait transition between two gait patterns that have different dynamic conditions.

Although phase resetting has been demonstrated to be useful in the generation of adaptive locomotion of legged robots [5], [6], [55–57], [84], our results show that phase resetting contributes to not only a single gait pattern but also to different gait patterns and their switching without incorporating special techniques. This further clarifies the usefulness of phase resetting in the generation of adaptive locomotion of legged robots and will lead to further progress in the design of a locomotion control system.

This paper employed synergy structures inspired from biological systems in the motion planning of our robot during the gait transition. Synergy structure seems to be a key to solving the redundancy problem in the designing of robot motion. For the synergy structure, we focused on the COM location and the trunk orientation, which are especially important parameters for various whole-body movements [28]. Our approach is not specific to our robot and task because the approach must be applicable to various robots and tasks using whole-body movements. In addition, humans and animals share some synergetic patterns between various movements in the generation of their movements and produce such various movements by adding other synergetic patterns, for example, jump, swim, and walk of frogs, and walk, obstacle avoidance, kick motion, and run of humans [15], [21], [41], [42]. To create such various movements of robots, constructing synergy structures and choosing the necessary structures depending on the task might be useful.

Physiological studies have investigated gait transition from quadrupedal to bipedal walking to elucidate the origin of bipedal walking. In particular, many studies experimented on these gait patterns using monkeys and examined the biomechanical and physiological differences in the control systems [51], [52], [54], [58], [59]. Animals generate highly coordinated and skillful motions by integrating nervous, sensory, and musculoskeletal systems. By synthesizing biomechanical and physiological knowledge, robotics research is expected to contribute to the elucidation of the mechanisms in motion generation and the control strategies, as well as to create new design principles for the control systems of legged robots.

Acknowledgment

The authors thank Dr. Katsuyoshi Tsujita for his help in the design of the biped robot and Mr. Takahiro Kondo for his help with the experiments. This paper is supported in part by a Grant-in-Aid for Scientific Research (B) No. 23360111 and a Grant-in-Aid for Creative Scientific Research No. 19GS0208 from the Ministry of Education, Culture, Sports, Science, and Technology of Japan.

References

[1] A.V. Alexandrov, A.A. Frolov, and J. Massion, *Axial synergies during human upper trunk bending*, Exp. Brain Res., 118:210–220, 1998.

[2] A.V. Alexandrov, A.A. Frolov, and J. Massion, *Biomechanical analysis of movement strategies in human forward trunk bending. I. Modeling*, Biol. Cyben., 84: 425–434, 2001.

[3] A.V. Alexandrov, A.A. Frolov, and J. Massion, *Biomechanical analysis of movement strategies in human forward trunk bending. II. Experimental study*, Biol. Cyben., 84: 435–443, 2001.

[4] S. Aoi, N. Ogihara, T. Funato, Y. Sugimoto, and K. Tsuchiya, *Evaluating functional roles of phase resetting in generation of adaptive human bipedal walking with a physiologically based model of the spinal pattern generator*, Biol. Cybern., 102(5):373–387, 2010.

[5] S. Aoi and K. Tsuchiya, *Locomotion control of a biped robot using nonlinear oscillators*, Auton. Robots, 19(3):219–232, 2005.

[6] S. Aoi and K. Tsuchiya, *Adaptive behavior in turning of an oscillator-driven biped robot*, Auton. Robots, 23(1):37–57, 2007.

[7] S. Aoi and K. Tsuchiya, *Stability analysis of a simple walking model driven by an oscillator with a phase reset using sensory feedback*, IEEE Trans. Robotics, 22(2):391–397, 2006.

[8] S. Aoi and K. Tsuchiya, *Self-stability of a simple walking model driven by a rhythmic signal*, Nonlinear Dyn., 48(1-2):1–16, 2007.

[9] S. Aoi and K. Tsuchiya, *Generation of bipedal walking through interactions among the robot dynamics, the oscillator dynamics, and the environment: Stability characteristics of a five-link planar biped robot*, Auton. Robots, 30(2):123–141, 2011.

[10] S. Aoi, T. Yamashita, and K. Tsuchiya, *Hysteresis in the gait transition of a quadruped investigated using simple body mechanical and oscillator network models*, Phys. Rev. E, 83(6):061909, 2011.

[11] K. Asa, K. Ishimura, and M. Wada, *Behavior transition between biped and quadruped walking by using bifurcation*, Robot. Auton. Syst., 57:155–160, 2009.

[12] L. Bianchi, D. Angelini, G.P. Orani, and F. Lacquaniti, *Kinematic coordination in human gait: Relation to mechanical energy cost*, J. Neurophysiol., 79:2155–2170, 1998.

[13] G. Bosco and R.E. Poppele, *Proprioception from a spinocerebellar perspective*, Physiol. Rev., 81:539–568, 2001.

[14] R.E. Burke, A.M. Degtyarenko, and E.S. Simon, *Patterns of locomotor drive to motoneurons and last-order interneurons: Clues to the structure of the CPG*, J. Neurophysiol., 86:447–462, 2001.

[15] G. Cappellini, Y.P. Ivanenko, R.E. Poppele, and F. Lacquaniti, *Motor patterns in human walking and running*, J. Neurophysiol., 95:3426–3437, 2006.

[16] J.J. Collins and I.N. Stewart, *Coupled nonlinear oscillators and the symmetries of animal gaits*, J. Nonlinear Sci., 3:349–392, 1993.

[17] B.A. Conway, H. Hultborn, and O. Kiehn, *Proprioceptive input resets central locomotor rhythm in the spinal cat*, Exp. Brain Res., 68:643–656, 1987.

[18] G. Courtine and M. Schieppati, *Human walking along a curved path. II. Gait features and EMG patterns*, Eur. J. Neurosci.:18(1):191–205, 2003.

[19] A. Crespi and A.J. Ijspeert, *Online optimization of swimming and crawling in an amphibious snake robot*, IEEE Trans. Robotics, 24:75–87, 2008.

[20] A. Danna-dos-Santos, K. Slomka, V.M. Zatsiorsky, and M.L. Latash, *Muscle modes and synergies during voluntary body sway*, Exp. Brain Res., 179:533–550, 2007.

[21] A. d'Avella and E. Bizzi, *Shared and specific muscle synergies in natural motor behaviors*, Proc. Natl. Acad. Sci. USA, 102(8):3076–3081, 2005.

[22] A. d'Avella, P. Saltiel, and E. Bizzi, *Combinations of muscle synergies in the construction of a natural motor behavior*, Nat. Neurosci., 6:300–308, 2003.

[23] J. Dean, T. Kindermann, J. Schmitz, M. Schumm, and H. Cruse, *Control of walking in the stick insect: From behavior and physiology to modeling*, Auton. Robots, 7:271–288, 1999.

[24] N. Dominici, Y.P. Ivanenko, G. Cappellini, A. d'Avella, V. Mondì, M. Cicchese, A. Fabiano, T. Silei, A. Di Paolo, C. Giannini, R.E. Poppele, and F. Lacquaniti, *Locomotor primitives in newborn babies and their development*, Science, 334:997–999, 2011.

[25] T. Drew, J. Kalaska, and N. Krouchev, *Muscle synergies during locomotion in the cat: a model for motor cortex control*, J. Physiol., 586(5):1239–1245, 2008.

[26] J. Duysens, *Fluctuations in sensitivity to rhythm resetting effects during the cat's step cycle*, Brain Res., 133(1):190–195, 1977.

[27] G. Endo, J. Morimoto, T. Matsubara, J. Nakanishi, and G. Cheng, *Learning CPG-based biped locomotion with a policy gradient method: Application to a humanoid robot*, Int. J. Robot. Res., 27(2):213–228, 2008.

[28] S.M.S.F. Freitas, M. Duarte, and M.L. Latash, *Two kinematic synergies in voluntary whole-body movements during standing*, J. Neurophysiol., 95: 636–645, 2006.

[29] T. Fukuda, Y. Hasegawat, M. Doi, and Y. Asano, *Multi-locomotion robot -Energy-based motion control for dexterous brachiation-*, Proc. IEEE Int. Conf. on Robot. Biomim., pp. 4–9, 2005.

[30] T. Funato, S. Aoi, H. Oshima, and K. Tsuchiya, *Variant and invariant patterns embedded in human locomotion through whole body kinematic coordination*, Exp. Brain Res., 205(4):497–511, 2010.

[31] A. Gams, A.J. Ijspeert, S. Schaal, and J. Lenarčič, *On-line learning and modulation of periodic movements with nonlinear dynamical systems*, Auton. Robots, 27:3–23, 2009.

[32] S.M. Gatesy and A.A. Biewener, *Bipedal locomotion: effects of speed, size and limb posture in birds and humans*, J. Zool. Lond., 224:127–147, 1991.

[33] T. Geng, B. Porr, and F. Wörgötter, *Fast biped walking with a sensor-driven neuronal controller and real-time online learning*, Int. J. Robot. Res., 25(3):243–259, 2006.

[34] A. Goswami, *Postural stability of biped robots and the foot-rotation indicator (FRI) point*, Int. J. Robot. Res., 18(6):523–533, 1999.

[35] S. Grillner, *Locomotion in vertebrates: central mechanisms and reflex interaction*, Physiol. Rev., 55(2):247–304, 1975.

[36] P. Guertin, M.J. Angel, M.-C. Perreault, and D.A. McCrea, *Ankle extensor group I afferents excite extensors throughout the hindlimb during fictive locomotion in the cat*, J. Physiol., 487(1):197–209, 1995.

[37] P.A. Guertin, *The mammalian central pattern generator for locomotion*, Brain Res. Rev., 62:45–56, 2009.

[38] A.L. Hof, M.G.J. Gazendam, and W.E. Sinke, *The condition for dynamic stability*, J. Biomech., 38:1–8, 2005.

[39] A.J. Ijspeert, A. Crespi, D. Ryczko, and J.M. Cabelguen, *From swimming to walking with a salamander robot driven by a spinal cord model*, Science, 315:1416–1420, 2007.

[40] A.J. Ijspeert, *Central pattern generators for locomotion control in animals and robots: a review*, Neural Netw., 21(4):642–653, 2008.

[41] Y.P. Ivanenko, R.E. Poppele, and F. Lacquaniti, *Five basic muscle activation patterns account for muscle activity during human locomotion*, J. Physiol., 556:267–282, 2004.

[42] Y.P. Ivanenko, R.E. Poppele, and F. Lacquaniti, *Motor control programs and walking*, Neuroscientist, 12(4):339–348, 2006.

[43] Y.P. Ivanenko, G. Cappellini, N. Dominici, R.E. Poppele, and F. Lacquaniti, *Coordination of locomotion with voluntary movements in humans*, J. Neurosci., 25(31):7238–7253, 2005.

[44] H. Kimura, Y. Fukuoka, and A. Cohen, *Adaptive dynamic walking of a quadruped robot on natural ground based on biological concepts*, Int. J. Robot. Res., 26(5):475–490, 2007.

[45] F. Lacquaniti, R. Grasso, and M. Zago, *Motor patterns in walking*, News Physiol. Sci., 14:168–174, 1999.

[46] M. Lafreniere-Roula and D.A. McCrea, *Deletions of rhythmic motoneuron activity during fictive locomotion and scratch provide clues to the organization of the mammalian central pattern generator*, J. Neurophysiol., 94:1120–1132, 2005.

[47] F.S. Labini, Y.P. Ivanenko, G. Cappellini, S. Gravano, and F. Lacquaniti, *Smooth changes in the EMG patterns during gait transitions under body weight unloading*, J. Neurophysiol. 106:1525–1536, 2011.

[48] J. Lee, S.N. Sponberg, O.Y. Loh, A.G. Lamperski, R.J. Full, and N.J. Cowan, *Templates and anchors for antenna-based wall following in cockroaches and robots*, IEEE Trans. Robotics, 24:130–143, 2008.

[49] M.J. MacLellan and B.J. McFadyen, *Segmental control for adaptive locomotor adjustments during obstacle clearance in healthy young adults*, Exp. Brain Res., 202(2):307–318, 2010.

[50] D.A. McCrea and I.A. Rybak, *Organization of mammalian locomotor rhythm and pattern generation*, Brain Res. Rev., 57:134–146, 2008.

[51] S. Mori, F. Mori, and K. Nakajima, *Higher nervous control of quadrupedal vs bipedal locomotion in non-human primates; Common and specific properties*, Adaptive Motion of Animals and Machines, H. Kimura, K. Tsuchiya, A. Ishiguro, and H. Witte (Eds.), pp. 53–65, Springer, 2006.

[52] F. Mori, A. Tachibana, C. Takasu, K. Nakajima, and S. Mori, *Bipedal locomotion by the normally quadrupedal Japanese monkey, M. Fuscata: strategies for obstacle clearance and recovery from stumbling*, Acta Physiol. Pharmacol. Bulg., 26(3):147–150, 2001.

[53] S.M. Morton and A.J. Bastian, *Cerebellar contributions to locomotor adaptations during splitbelt treadmill walking*, J. Neurosci., 26(36):9107–9116, 2006.

[54] K. Nakajima, F. Mori, C. Takasu, M. Mori, K. Matsuyama, and S. Mori, *Biomechanical constraints in hindlimb joints during the quadrupedal versus bipedal locomotion of M. fuscata*, Prog. Brain Res., 143: 183-190, 2004.

[55] J. Nakanishi, J. Morimoto, G. Endo, G. Cheng, S. Schaal, and M. Kawato, *Learning from demonstration and adaptation of biped locomotion*, Robot. Auton. Syst., 47(2-3):79–91, 2004.

[56] M. Nakanishi, T. Nomura, and S. Sato, *Stumbling with optimal phase reset during gait can prevent a humanoid from falling*, Biol. Cybern., 95:503–515, 2006.

[57] T. Nomura, K. Kawa, Y. Suzuki, M. Nakanishi, and T. Yamasaki, *Dynamic stability and phase resetting during biped gait*, Chaos, 19:026103, 2009.

[58] N. Ogihara, S. Aoi, Y. Sugimoto, K. Tsuchiya, and M. Nakatsukasa, *Forward dynamic simulation of bipedal walking in the Japanese macaque: investigation of causal relationships among limb kinematics, speed, and energetics of bipedal locomotion in a non-human primate*, Am. J. Phys. Anthropol., 145(4):568-580, 2011.

[59] N. Ogihara, H. Makishima, S. Aoi, Y. Sugimoto, K. Tsuchiya, and M. Nakatsukasa, *Development of an anatomically based whole-body musculoskeletal model of the Japanese macaque (Macaca fuscata)*, Am. J. Phys. Anthropol., 139(3):323–338, 2009.

[60] G.N. Orlovsky, T. Deliagina, and S. Grillner, Neuronal control of locomotion: from mollusc to man, *Oxford University Press*, 1999.

[61] K. Pearson, Ö. Ekeberg, and A. Büschges, *Assessing sensory function in locomotor systems using neuro-mechanical simulations*, Trends. Neurosci., 29(11):625–631, 2006.

[62] R. Pfeifer, M. Lungarella, and F. Iida, *Self-organization, embodiment, and biologically inspired robotics*, Science, 318:1088–1093, 2007.

[63] R.E. Poppele, G. Bosco, and A.M. Rankin, *Independent representations of limb axis length and orientation in spinocerebellar response components*, J. Neurophysiol., 87:409–422, 2002.

[64] R.E. Poppele and G. Bosco, *Sophisticated spinal contributions to motor control*, Trends. Neurosci., 26:269–276, 2003.

[65] D.S. Reisman, H.J. Block, and A.J. Bastian, *Interlimb coordination during locomotion: What can be adapted and stored?*, J. Neurophysiol., 94:2403–2415, 2005.

[66] L. Ren and J.R. Hutchinson, *The three-dimensional locomotor dynamics of African (Loxodonta africana) and Asian (Elephas maximus) elephants reveal a smooth gait transition at moderate speed*, J. R. Soc. Interface, 5:195–211, 2008.

[67] R.E. Ritzmann, R.D. Quinn, and M.S. Fischer, *Convergent evolution and locomotion through complex terrain by insects, vertebrates and robots*, Arthropod Struct. Dev., 33:361–379, 2004.

[68] S. Rossignol, R. Dubuc, and J. Gossard, *Dynamic sensorimotor interactions in locomotion*, Physiol. Rev., 86:89–154, 2006.

[69] J. Rubenson, D.B. Heliams, D.G. Lloyd, and P.A. Fournier, *Gait selection in the ostrich: mechanical and metabolic characteristics of walking and running with and without an aerial phase*, Proc. R. Soc. Lond. B, 271:1091–1099, 2004.

[70] I.A. Rybak, N.A. Shevtsova, M. Lafreniere-Roula, and D.A. McCrea, *Modelling spinal circuitry involved in locomotor pattern generation: insights from deletions during fictive locomotion*, J. Physiol., 577(2):617–639, 2006.

[71] I.A. Rybak, K. Stecina, N.A. Shevtsova, and D.A. McCrea, *Modelling spinal circuitry involved in locomotor pattern generation: insights from the effects of afferent stimulation*, J. Physiol., 577(2):641–658, 2006.

[72] S. Schaal, *Is imitation learning the route to humanoid robots?*, Trends. Cogn. Sci., 3:233–242, 1999.

[73] S. Schaal, A. Ijspeert, and A. Billard, *Computational approaches to motor learning by imitation*, Phil. Trans. R. Soc. Lond. B, 358:537–547, 2003.

[74] E.D. Schomburg, N. Petersen, I. Barajon, and H. Hultborn, *Flexor reflex afferents reset the step cycle during fictive locomotion in the cat*, Exp. Brain Res., 122(3):339–350, 1998.

[75] G. Schtner, W.Y. Jiang, and J.A.S. Kelso, *A synergetic theory of quadrupedal gaits and gait transitions*, J. Theor. Biol., 142:359–391, 1990.

[76] M.L. Shik and G.N. Orlovsky, *Neurophysiology of locomotor automatism*, Phsyiol. Rev., 56(3):465–501, 1976.

[77] S. Steingrube, M. Timme, F. Wörgötter, and P. Manoonpong, *Self-organized adaptation of a simple neural circuit enables complex robot behaviour*, Nat. Phys., 6:224–230, 2010.

[78] G. Taga, Y. Yamaguchi, and H. Shimizu, *Self-organized control of bipedal locomotion by neural oscillators in unpredictable environment*, Biol. Cybern., 65: 147–159, 1991.
[79] G. Taga, *A model of the neuro-musculo-skeletal system for human locomotion I. Emergence of basic gait*, Biol. Cybern., 73: 97–111, 1995.
[80] G. Taga, *A model of the neuro-musculo-skeletal system for human locomotion II. - Real-time adaptability under various constraints*, Biol. Cybern., 73: 113–121, 1995.
[81] K. Takakusaki and T. Okumura, *Neurobiological basis of controlling posture and locomotion*, Adv. Robot., 22:1629–1663, 2008.
[82] L.H. Ting and J.M. Macpherson, *A limited set of muscle synergies for force control during a postural task*, J. Neurophysiol., 93:609–613, 2005.
[83] E. Todorov and M.I. Jordan, *Optimal feedback control as a theory of motor coordination*, Nat. Neurosci., 5:1226–1235, 2002.
[84] K. Tsujita, K. Tsuchiya, and A. Onat, *Adaptive gait pattern control of a quadruped locomotion robot*, Proc. IEEE/RSJ Int. Conf. on Intell. Robots Syst., pp. 2318–2325, 2001.
[85] M. Vukobratović, B. Borovac, D. Surla, and D. Stokić, Biped locomotion-dynamics, stability, control and application, *Springer-Verlag*, 1990.
[86] S. Yakovenko, V. Gritsenko, and A. Prochazka, *Contribution of stretch reflexes to locomotor control: A modeling study*, Biol. Cybern., 90:146–155, 2004.
[87] T. Yamasaki, T. Nomura, and S. Sato, *Possible functional roles of phase resetting during walking*, Biol. Cybern., 88:468–496, 2003.

PLACE PHOTO HERE

Shinya Aoi received the B.E., M.E., and Ph.D. degrees from the Department of Aeronautics and Astronautics, Kyoto University, Kyoto, Japan in 2001, 2003, and 2006, respectively.

From 2003 to 2006, he was a Research Fellow of the Japan Society for the Promotion of Science (JSPS). From 2006 to 2007, he was a COE Assistant Professor at Kyoto University. Since 2007, has been an Assistant Professor in the Department of Aeronautics and Astronautics, Graduate School of Engineering, Kyoto University. His research interests include dynamics and control of robotic systems, especially legged robots, and analysis and simulations of locomotion in humans and animals.

PLACE PHOTO HERE

Yoshimasa Egi was a master course student of the Department of Aeronautics and Astronautics, Kyoto University, Kyoto, Japan. He received the B.E. and M.E. degrees from Kyoto University in 2007 and 2009, respectively.

He is now working at Okuma Corporation, Aichi, Japan. His research interests include the control of legged robots.

PLACE PHOTO HERE

Ryuichi Sugimoto was a master course student of the Department of Aeronautics and Astronautics, Kyoto University, Kyoto, Japan. He received the B.E. and M.E. degrees from Kyoto University in 2007 and 2009, respectively.

He is now working at Sony Corporation, Tokyo, Japan. His research interests include the control of legged robots.

PLACE PHOTO HERE

Tsuyoshi Yamashita was a master course student of the Department of Aeronautics and Astronautics, Kyoto University, Kyoto, Japan. He received the B.E. and M.E. degrees from Kyoto University in 2009 and 2011, respectively.

He is now working at Mitsubishi Electric, Kamakura, Japan. His research interests include the control of legged robots.

PLACE PHOTO HERE

Soichiro Fujiki received the B.E. and M.E. degrees from the Department of Aeronautics and Astronautics, Kyoto University, Kyoto, Japan in 2010 and 2012, respectively.

He is now a doctor course student of the Department of Aeronautics and Astronautics, Kyoto University, Kyoto, Japan. His research interests include the control of legged robots.

PLACE PHOTO HERE

Kazuo Tsuchiya received the B.S., M.S., and Ph.D. degrees in Engineering from Kyoto University, Kyoto, Japan in 1966, 1968, and 1975, respectively.

From 1968 to 1990, he was a research member of the Central Research Laboratory at Mitsubishi Electric Corporation, Amagasaki, Japan. From 1990 to 1995, he was a Professor at the Department of Computer Controlled Machinery, Osaka University, Osaka, Japan. From 1995 to 2007, he was a Professor at the Department of Aeronautics and Astronautics, Kyoto University. In 2007, he retired from Kyoto University and became a Professor Emeritus of Kyoto University. Since 2008, he has been a Professor at the Department of Mechanical Engineering, Doshisha University. In 2011, he received the Asahi Prize for Spacecraft “Hayabusa” Project Team as a representative of academia. His fields of research include dynamic analysis, guidance, and control of space vehicles, and nonlinear system theory for distributed autonomous systems.